

## 7.4 QUADRANT ANALYSIS OF THE SCALAR AND MOMENTUM FLUXES IN THE MARINE ATMOSPHERIC SURFACE LAYER

George Katsouvas<sup>1</sup>, Costas G. Helmis<sup>1,\*</sup> and Qing Wang<sup>2</sup>

<sup>1</sup>Department of Applied Physics,  
Faculty of Physics, University of Athens, Greece

<sup>2</sup>Department of Meteorology,  
Naval Postgraduate School, Monterey, CA, USA

### 1. INTRODUCTION

Quadrant analysis, among other conditional sampling techniques, has been extensively used in the study and description of turbulent shear flows near rough and smooth boundaries (Antonia, 1981; Willmarth and Lu, 1974). This technique allocates momentum and/or scalar transport into four different types of events, which can be considered as the foundation of coherent structures in the turbulent flow (Cantwell, 1981; Robinson, 1991). Direct comparisons with turbulent flow visualization have shown that the quadrant technique exhibits great reliability in providing correct quantitative data in support of the visual observations (Bogard and Tiederman, 1986). The turbulent fluxes of latent heat, sensible heat, and momentum near the surface for different terrain types have been often described in terms of the quadrant analysis (Shaw et al, 1983; Katul et al, 1997; Hogstrom and Bergstrom, 1996). In the present work the quadrant technique is applied to marine boundary layer data collected during the 2003 experimental campaign in the frame of the Coupled Boundary Layer Air – Sea Transfer, Low wind component (CBLAST-Low), at Nantucket Island, Massachusetts. Both heat and momentum transfers are studied using quadrant analysis for different meteorological conditions.

### 2. EXPERIMENTAL SETUP

The three wind components ( $u$ ,  $v$  and  $w$ ) and the virtual temperature ( $T$ ) were sampled by two sonic anemometers at 10 m and 20 m height. All these variables were sampled at 20Hz and are used for the calculation of both momentum ( $u'w'$  and  $v'w'$ ) and scalar flux ( $w'T'$ ), under varying

stability and wind speed conditions. These measurements were conducted from 30 July 2003 to 27 August, at a distance of 90 meters from the shoreline over relatively flat terrain. Since an Internal Boundary Layer (IBL) is expected to develop reaching the depth of 10 meters, in most of the cases, the data concerning the Marine Surface Layer (MSL) was carefully separated from the whole data set, as will be described in the next section.

### 3. METHODOLOGY

#### 3.1 Data Correction and Processing

A few correction/selection procedures were applied to the dataset before the analysis. The first one was the correction due to the axis tilt of the anemometer. To do this, ten minutes averages of the three wind components ( $u$ ,  $v$  and  $w$ ), calculated in the sonic coordinate system, for a 28 days time period, were utilized. This correction was aimed at eliminating the dependence of  $\overline{w}$  on both  $\overline{u}$  and  $\overline{v}$ , which is expected to arise due to the tilt of the anemometer from the true vertical. Although the calculated rotation angles were relatively small ( $\vartheta_1 = -0.063$  degrees and  $\vartheta_2 = -2.486$  degrees) the influence of the correction was quite important, especially for the low wind speed range. Suggestively, the relative difference between the initial value of  $u^*$  and the corrected one, can exceed 50%.

Furthermore, the non-stationary cases were excluded from the analysis, according to the methodology described by Mahrt et al., 1996. The classification of a case as stationary or non-stationary was based on the value of the ratio:

$$\beta = \frac{(\sigma_u^2 + \sigma_v^2)^{\frac{1}{2}}}{\overline{U}} \quad (1)$$

where the standard deviations are computed from the six 10-minute average of the wind components for 1-hour period and  $\overline{U}$  is the 1-hour averaged wind speed. If the hourly value of

---

*Corresponding author address:* Costas G. Helmis, University of Athens, Department of Applied Physics, University Campus, Building Phys.-5, 15784, Athens, GREECE, e-mail: chelmis@cc.uoa.gr

$\beta$  exceeds 0.1, the case is identified as non-stationary and it is excluded from the analysis.

Finally, as mentioned before, the data corresponding to the MSL were separated from the IBL influenced data, for the 20 meters height level. The marine data set was defined through a detailed examination of the measured momentum and heat flux, and the stability parameter ( $-z/L$ ) time series at both 10 m and 20 m levels. A typical marine case for the 20 meters height level is given in Fig. 1. From this figure it's evident that stable stratification prevails at the level of 20 m height (gray line) for the whole day, which is combined with constantly negative values of heat flux (blue line). The conditions at this level stay unaffected by the development of the island's internal boundary layer, which is indicated by the raise of the heat flux (red line) and the unstable conditions (black line) at the level of 10m, during the midday. Thus, in this case, sensors at 20 meters height constantly measure the marine boundary layer.

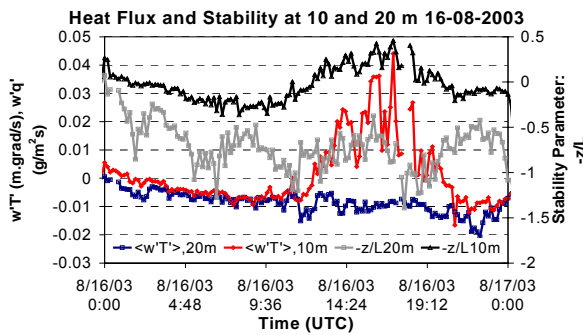


Figure 1: The sensible heat fluxes at 20 m (blue line) and at 10 m (red line), and stability parameter at 20 m and 10 m (gray and black lines, respectively) time series for a typical marine case.

### 3.2 Quadrant Analysis

Quadrant analysis provides information on the process of turbulent production and transfer by sorting the instantaneous values of the Reynolds stress  $u'w'$  into four categories according to the sign of the two fluctuating components. The quadrants in the  $(u', w')$ -plane are numbered conventionally and named as follows (Shaw et al., 1983):

- Quadrant 1:  $u' > 0, w' > 0$  outward interaction
- Quadrant 2:  $u' < 0, w' > 0$  ejection or burst
- Quadrant 3:  $u' < 0, w' < 0$  inward interaction
- Quadrant 4:  $u' > 0, w' < 0$  sweep or gust

Quadrant definitions for momentum transfer are depicted in figure 2.

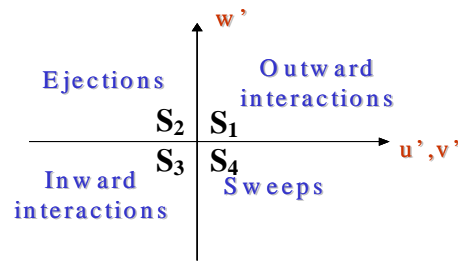


Figure 2: Quadrant definitions for momentum flux.

Quadrants 2 and 4 both correspond to downward diffusion of momentum and quadrants 1 and 3 each represent upward transfer. The hyperbola:

$$|u'w'| = H |\overline{u'w'}| \quad (2)$$

defines a fifth area in the  $(u'w')$ -plane for the conditional analysis and it is used to separate the most important events, with large values of  $|u'w'|$ , from the less important ones. According to Raupach (1981) a stress fraction  $S_{i,H}$  is defined as:

$$S(i, H) = \frac{\langle w'u' \rangle_{i,H}}{\overline{w'u'}} \quad (3)$$

where the subscript  $i$  corresponds to the quadrant number and

$$\langle u'w' \rangle_{i,H} = \lim_{T \rightarrow \infty} \frac{1}{T} \int_0^T u'w'(t) I_{i,H}(t) dt \quad (4)$$

is a conditional average, since the term  $I_{i,H}$  is the following conditioning function:

$$I_{i,H} = \begin{cases} 0, & \text{if } u'w' \text{ is in quad. } i \text{ and } |u'w'| \geq H |\overline{u'w'}| \\ 1, & \text{otherwise} \end{cases} \quad (5)$$

From the definition of the stress fraction easily arises that:

$$\sum_{i=1}^4 S_{i,0} = 1 \quad (6)$$

The total time that is occupied by a specific event within the Reynolds stress averaging time is called fractional time  $T_{i,H}$  and it is defined as:

$$T_{i,H} = \frac{1}{T} \int_0^T I_{i,H}(t) dt \quad (7)$$

The ratio of upward to downward momentum transfer (E):

$$E = \frac{S_{1,0} + S_{3,0}}{S_{2,0} + S_{4,0}} \quad (8)$$

was introduced by Shaw et al. (1983) and was called the exuberance, since it represents a measure of the upward momentum transfer, which is counter to the overall downward flux, expressing the exuberant nature of the flow.

The definitions of the four quadrants for the scalar transport (e.g.  $w'T'$  or  $w'q'$ ) are altered compared to the previous definitions for momentum flux and are briefly described in figure 3 (see also Katul et al., 1997 for the quadrant nomenclature for scalar transport).

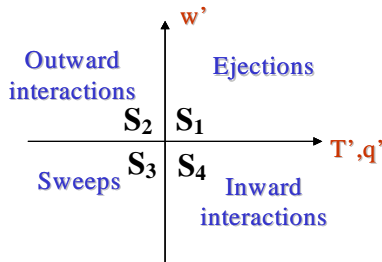


Figure 3: Quadrant definitions for scalar transport.

Regarding the heat transfer ( $w'T'$ ), it is worth noting that ejections and sweeps become the dominant quadrants for unstable conditions, while for stable stratification the interaction quadrants prevail, in consistency to upward and downward overall heat transfer, respectively.

#### 4. RESULTS AND DISCUSSION

The following section includes the results of the  $u'w'$ ,  $v'w'$  and  $w'T'$  covariance analysis under the scope of quadrant analysis. From total 28 days of continuous data, only the marine data that correspond to stationary cases (see section 3.1) and stable conditions are analyzed. All covariances are calculated for a 10-minute time scale.

##### 4.1 $u'w'$ covariance

In figures 4, 5 and 6 the stress fraction ( $S_i$ ) of each quadrant is plotted as a function of the wind speed, the stability parameter ( $-z/L$ ) and the normalized momentum flux ( $\overline{u'w'}/U^2$ ),

respectively. The definitions described in figure 2 are retained in figures 4, 5 and 6.

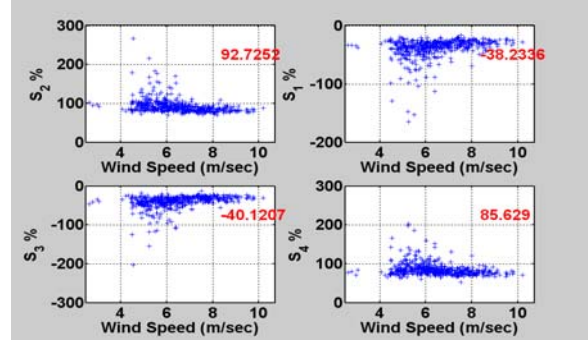


Figure 4: The flux fraction of each quadrant as a function of the wind speed. The characters in red represent the mean value.

It's concluded that there is a slight increase of the absolute value of all quadrants for low winds. It is also apparent that the contribution to the total flux from Ejections ( $S_2$ ) and Sweeps ( $S_4$ ) is significantly larger (93% and 86%, respectively) than that from the interaction quadrants (-38% for outward interactions and -40% for inward interactions). Furthermore, as shown in figures 5 and 6, the flux fraction's absolute value of all quadrants is clearly decreasing with decreasing stability and with increasing normalized momentum flux ( $\overline{u'w'}/U^2$ ).

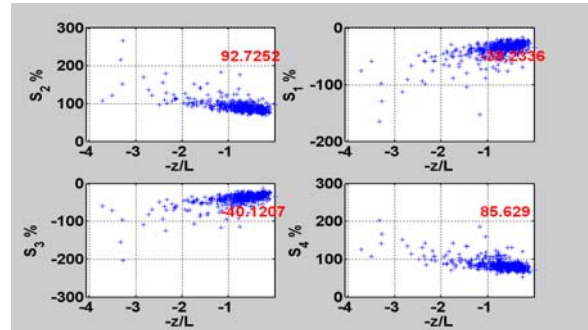


Figure 5: The flux fraction of each quadrant as a function of the stability parameter ( $-z/L$ ). The characters in red represent the mean value.

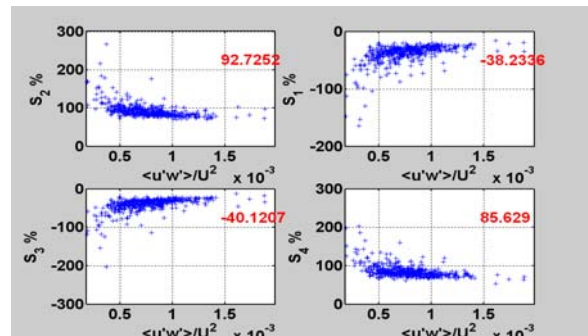


Figure 6: The flux fraction of each quadrant as a function of the normalized momentum flux. The characters in red represent the mean value.

Figures 7, 8 and 9 depict the flux exuberance against the wind speed, the stability parameter and the normalized momentum flux, respectively. Flux exuberance is enhanced for increasing stability and for low normalized momentum flux values, while it's slightly increasing for decreasing wind speed. The same results stand for the time exuberance (not shown here), which can be defined as the sum of the time fractions for quadrants 1 and 3 to the sum of the time fractions of quadrants 2 and 4.

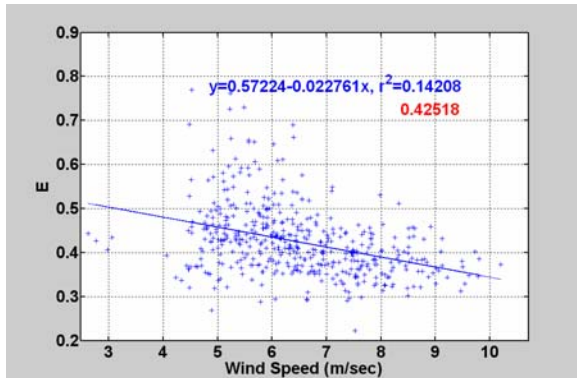


Figure 7: The exuberance as a function of the wind speed. The characters in red represent the mean value.

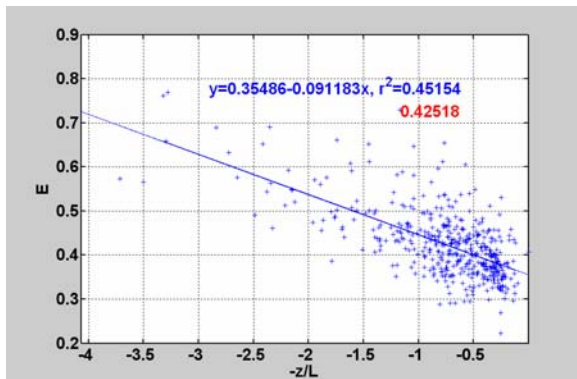


Figure 8: The exuberance as a function the stability parameter. The characters in red represent the mean value.

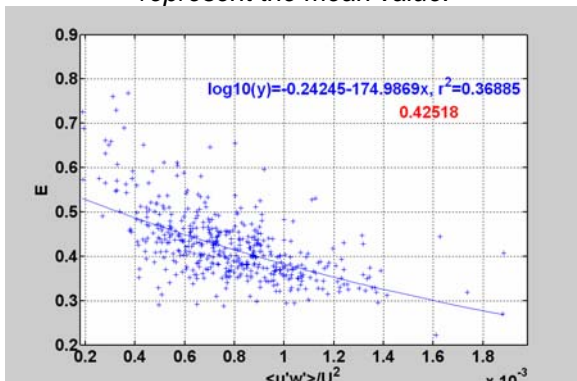


Figure 9: The exuberance as a function of the normalized momentum flux. The characters in red represent the mean value.

#### 4.2 $v'w'$ covariance

In figures 10, 11 and 12 the stress fraction ( $S_i$ ) of each quadrant is plotted as a function of the wind speed, the stability parameter and the normalized momentum flux ( $\overline{u'w'}/U^2$ ), respectively. The definitions described in figure 2 are retained in figures 10, 11 and 12. It is apparent that the stress fractions are almost independent of the wind speed, the stability parameter and the normalized momentum flux and that their absolute value can be extremely large due to the small mean value of the  $\overline{v'w'}$  covariance. Also, the sign of each stress fraction can be either positive or negative depending to the sign of the  $\overline{v'w'}$  covariance.

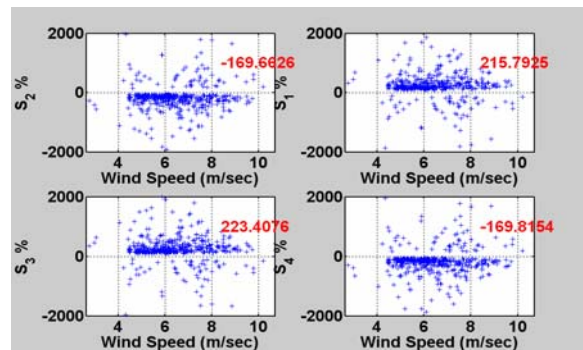


Figure 10: As in figure 4, but for the  $v'w'$  covariance.

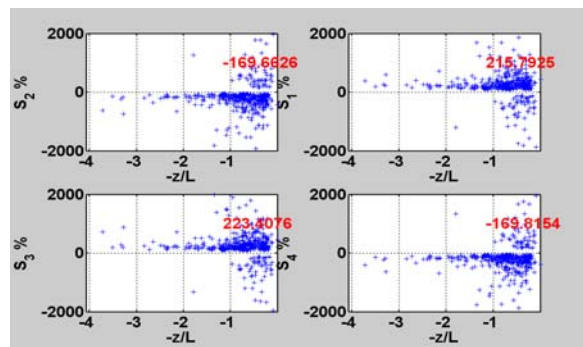


Figure 11: As in figure 5, but for the  $v'w'$  covariance.

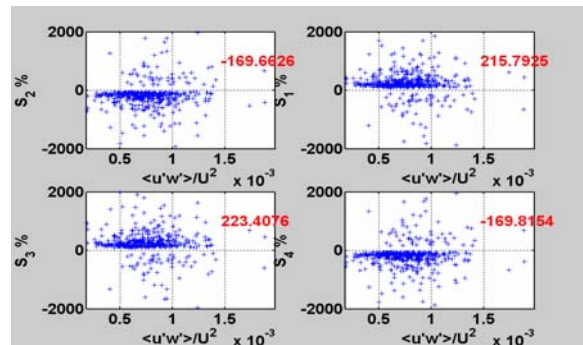


Figure 12: As in figure 6, but for the  $v'w'$  covariance.

The flux exuberance against the wind speed, the stability parameter and the normalized momentum flux is presented in figures 13, 14 and 15, respectively. The large scatter of the data does not permit the exclusion of certain conclusions; however the exuberance seems to have high values for low winds, for small values of normalized momentum flux and for stable conditions. Moreover, the mean value of exuberance is above unity implying the dominant role of the interaction quadrants against ejections and sweeps.

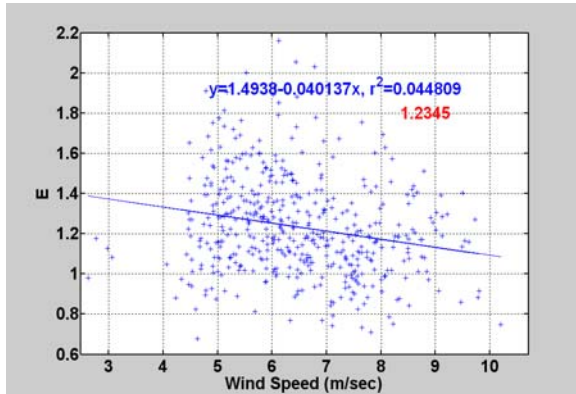


Figure 13: As in figure 7, but for the  $v'w'$  covariance.

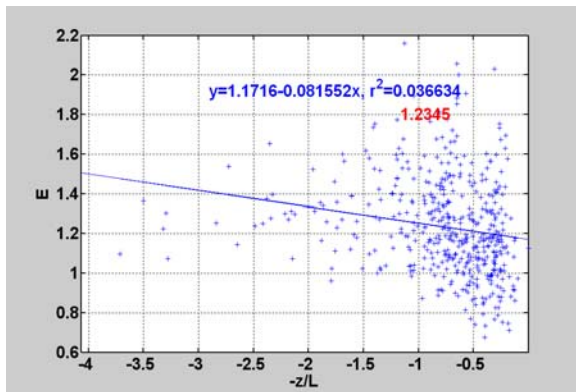


Figure 14: As in figure 8, but for the  $v'w'$  covariance.

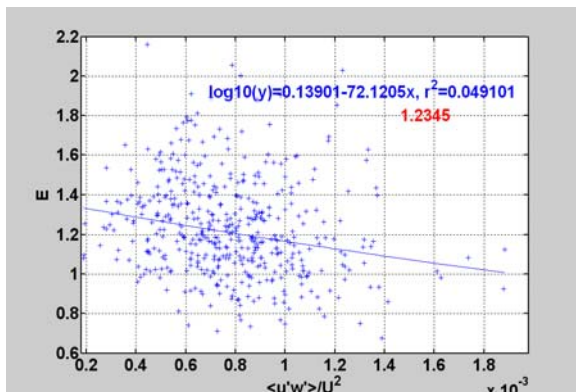


Figure 15: As in figure 9, but for the  $v'w'$  covariance.

### 4.3 $w'T'$ covariance

In figures 16, 17 and 18 the stress fraction ( $S_i$ ) of each quadrant is plotted as a function of the wind speed, the stability parameter ( $-z/L$ ) and the normalized momentum flux ( $\overline{u'w'}/U^2$ ), respectively. The definitions described in figure 3 are retained in figures 16, 17 and 18. As expected for stable stratification, the two interaction quadrants dominate the heat transfer process (77% for outward interactions and 82% for inward interactions). The absolute value of the stress fraction of all quadrants is increased for small momentum transfer, for low winds and for stable conditions.

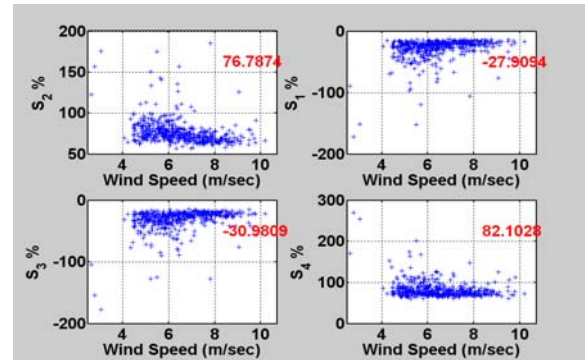


Figure 16: As in figure 4, but for the  $w'T'$  covariance.

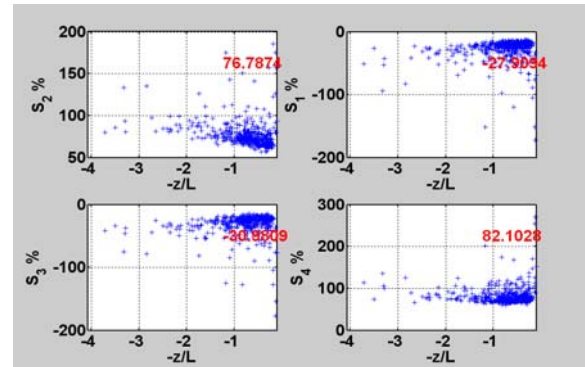


Figure 17: As in figure 5, but for the  $w'T'$  covariance.

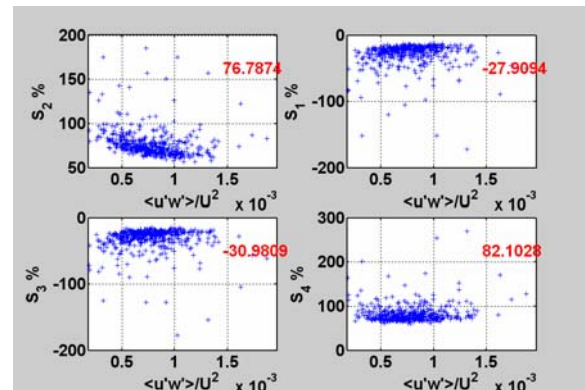


Figure 18: As in figure 6, but for the  $w'T'$  covariance.

The flux exuberance against the wind speed, the stability parameter and the normalized momentum flux is presented in figures 19, 20 and 21, respectively. The data exhibit large scatter, thus it is difficult to derive certain conclusions. Nevertheless, the exuberance seems to increase for increasing wind speed, for increasing normalized momentum flux and for near neutral conditions. Also, the mean value of exuberance is much above unity in consistency to the stable stratification.

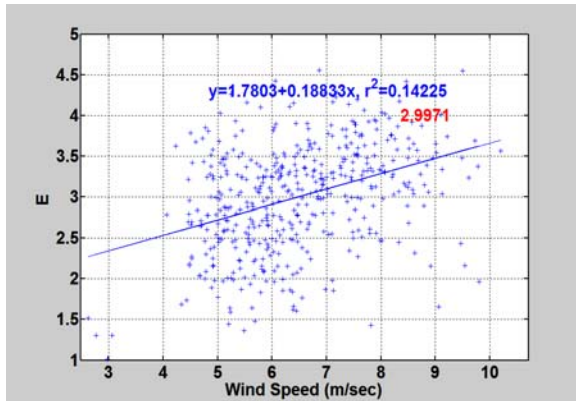


Figure 19: As in figure 7, but for the  $w'T'$  covariance.

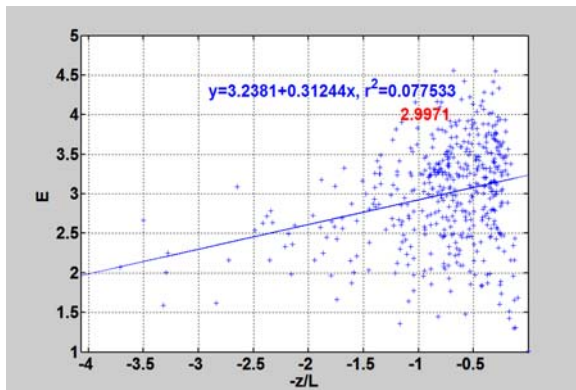


Figure 20: As in figure 8, but for the  $w'T'$  covariance.

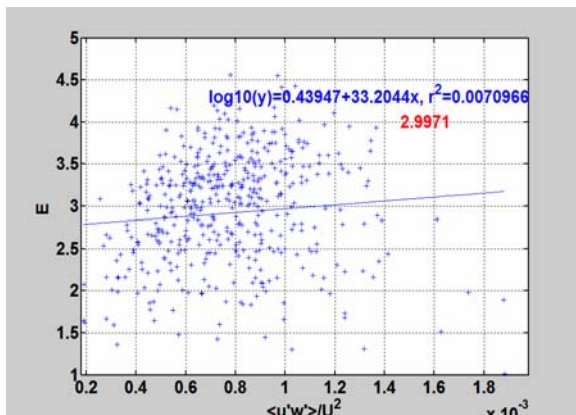


Figure 21: As in figure 9, but for the  $w'T'$  covariance.

## 5. CONCLUDING REMARKS

Quadrant analysis, applied on the stable and stationary marine data of the CBLAST-Low experiment, revealed the following:

- 1) Ejections and sweeps are the dominant processes of the  $u'w'$  momentum transfer, while inward and outward interactions prevail both in the  $v'w'$  covariance and in the  $w'T'$  covariance.
- 2) The exuberance is constantly below unity for the  $u'w'$  covariance (mean value = 0.43), implying that the role of unorganized motions is constricted. The opposite behavior is observed at the  $v'w'$  covariance, where the interaction quadrants prevail (mean value of Exuberance = 1.23). Regarding the  $w'T'$  covariance the exuberance is much above unity in all cases (mean value = 3) in consistency to the stable stratification and the downward overall heat transfer in the MSL.
- 3) Uncorrelated motions seem to affect the  $u'w'$  covariance more substantially for low winds, small values of normalized momentum transfer and very stable stratification. Under the same conditions the relative importance of ejections and sweeps in the  $w'T'$  covariance is increased. On the other hand, for the  $v'w'$  covariance, ejections and sweeps tend to balance the interaction quadrants for strong winds, large values of normalized momentum transfer and near neutral conditions.

## 6. ACKNOWLEDGMENTS

This work was supported by IRAKLEITOS Fellowships for Research of the Hellenic Ministry of Education and by the Office of Naval Research (Contract No N62558-03-M-0532 and its supplemental award N62558-04-P-6010).

## 7. REFERENCES

- Antonia, R. A., 1981: Conditional sampling in turbulence measurements. *Ann. Rev. Fluid Mech.*, **13**, 131-156.
- Bogard, D. G. and Tiederman, W. G., 1986: Burst detection with single-point velocity measurements. *J. Fluid Mech.*, **162**, 389-413.
- Cantwell, B., 1981: Organized motion in turbulent flow. *Ann. Rev. Fluid Mech.*, **13**, 457-515.

Hogstrom, U. and Bergstrom, H., 1996: Organized turbulence structures in the near-neutral atmospheric surface layer. *J. Atmos. Sci.*, **53**, 2452-2464.

Katul, G., Kuhn, G., Schieldge, J. and Hsieh, C.-I., 1997: The ejection-sweep character of scalar fluxes in the unstable surface layer. *Boundary-Layer Meteorol.*, **83**, 1-26.

Mahrt, L., Vickers, D., Howell, J., Hojstrup, J., Wilczak, J., Edson, J. and Hare J., 1996: Sea surface drag coefficients in the Riso Air Sea Experiment. *J. Geophys. Res.*, **101**, 14,327-14,335.

Robinson, S.K., 1991: Coherent motions in the turbulent boundary layer. *Ann. Rev. Fluid Mech.*, **23**, 601-639.

Shaw, R. H., Tavangar, J., and Ward, D. P., 1983: Structure of Reynolds stress in a canopy layer. *J. Clim. Appl. Meteorol.*, **22**, 1922-1931.

Willmarth, W. W. and Lu, S. S., 1974: Structure of the Reynolds stress and the occurrence of bursts in the turbulent boundary layer. *Adv. Geophys.*, **18A**, 287-314.